Intravesical combination treatment with antisense oligonucleotides targeting heat shock protein-27 and HTI-286 as a novel strategy for high-grade bladder cancer

Yoshiyuki Matsui,[1] Boris A. Hadaschik,[1] Ladan Fazli,[1] Raymond J. Andersen,[3] Martin E. Gleave,[1,2] and Alan I. So[1,2]

[1]The Prostate Centre at Vancouver General Hospital and Departments of [2]Urologic Sciences and [3]Earth and Ocean Sciences, University of British Columbia, Vancouver, British Columbia, Canada

Abstract

Clinical results of current intravesical chemotherapeutics are insufficient, and novel and safe intravesical options for high-risk bladder cancer are required to prevent both recurrence and progression. In this study, we show promising efficacy of intravesical combination treatment using antisense oligonucleotides targeting heat shock protein-27 (Hsp27; OGX427) with HTI-286, a synthetic analogue of the marine sponge product hemiasterlin. The expression of Hsp27 in bladder cancer was examined using tissue microarray analysis. Then, four bladder cancer cell lines were screened for combination effects of OGX427 with HTI-286, and the molecular mechanisms underlying the synergic effect were analyzed. Chemosensitivity against HTI-286 was also compared between mock-transfected T24 (T24 mock) cells and Hsp27-overexpressing T24 (T24 Hsp27) cells. Furthermore, *in vivo* data were obtained in a bioluminescent orthotopic murine model of high-grade disease. Hsp27 is expressed at higher levels in bladder cancers compared with normal bladder epithelium. OGX427 significantly enhanced cytotoxicity of HTI-286. Combination treatment induced Akt inactivation and Bcl-2 down-regulation. T24 Hsp27 cells were more resistant to HTI-286 than T24 mock cells and showed stronger Akt activation after HTI-286 treatment. The protective effect of Hsp27 against HTI-286 was suppressed by LY294002, a phosphatidylinositol 3-kinase inhibitor, indicating that Hsp27-Akt interactions are key mechanisms to enhance chemosensitivity via OGX427. Intravesical combination therapy effectively inhibited orthotopic tumor growth without toxic side effects. Our results suggest that OGX427 enhances cytotoxicity of HTI-286 through Akt inactivation and provide strong preclinical proof-of-principle for intravesical administration of OGX427 in combination with HTI-286 for high-grade bladder cancer. [Mol Cancer Ther 2009;8(8):2402–11]

Introduction

Bladder cancer, the fourth most common male cancer, is a significant clinical and economic burden with >68,000 cases diagnosed in the United States in 2008 (1). Approximately 70% of bladder cancers are non-muscle-invasive at initial diagnosis (2). Unfortunately, although transurethral resection is the primary treatment option for non-muscle-invasive bladder tumors, adjuvant treatment options, including intravesical therapy, are limited in prevention of tumor recurrence or progression. Despite intravesical chemotherapy and/or immunotherapy, ~80% of patients with non-muscle-invasive bladder cancer may develop recurrent tumors, of which 20% to 30% progress into more aggressive and potentially lethal tumors (3–5). Further, although immunotherapy with Bacillus Calmette-Guerin (BCG) has shown significant benefits for tumor prophylaxis compared with current intravesical chemotherapeutics (6), it is associated with significant local or systemic adverse effects and still >30% of high-risk patients ultimately require cystectomy within 15 years (4). Therefore, novel and safe intravesical options for early-stage high-risk bladder cancer are required to prevent both recurrence and progression.

We have developed several potential candidates for the intravesical treatment of noninvasive bladder cancer using a validated bioluminescent orthotopic murine model of high-grade disease (7–11). One of these is HTI-286, a fully synthetic analogue of the natural tripeptide hemiasterlin, which binds to the tubulin heterodimer at a unique site and interferes with spindle-microtubule dynamics at very low concentrations (12–17). HTI-286 is advantageous when compared with taxanes or conventional chemotherapeutic agents against bladder cancer including mitomycin C, because it is a poor substrate for P-glycoprotein (MDR1) and thus reduces the possibility of multidrug resistance (18). Several preclinical studies showed promising results, and an open-label phase I trial has been completed in patients with advanced solid tumors (12, 18–20). Intravesical HTI-286 treatment in our xenograft model showed promising antitumor activity with minimal toxicity (8). However, because high-performance liquid

Received 2/20/09; revised 5/5/09; accepted 5/19/09; published OnlineFirst 7/21/09.

Requests for reprints: Alan I. So, Department of Urologic Sciences, University of British Columbia, Gordon & Leslie Diamond Health Care Centre, 2775 Laurel Street, Level 6, Vancouver, British Columbia, Canada V5Z 1M9. Phone: 604-875-5006; Fax: 604-875-5654. E-mail: dralanso@interchange.ubc.ca

doi:10.1158/1535-7163.MCT-09-0148

chromatography-mass spectrometry detected systemic uptake after intravesical instillation of HTI-286, improvement of safety and tolerability of intravesically administered HTI-286 might be possible if the dose of HTI-286 can be further minimized.

Another promising candidate for intravesical therapy is antisense oligonucleotide (ASO) therapy targeting heat shock protein-27 (Hsp27; ref. 9). Hsp27 is a potent tumor survival chaperone protein, and its expression has been associated with treatment resistance and apoptosis among many tumors (21, 22). However, the functional significance of its expression in bladder cancer is still controversial (23, 24). Inhibition of Hsp27 was reported to enhance several chemotherapeutic agents such as cisplatinum and 17-allylamino-demethoxygeldanamycin, and we have shown previously that a systemically delivered ASO targeting Hsp27 (OGX427; OncoGeneX) potently enhanced sensitivity to paclitaxel in s.c. xenograft model of bladder and prostate cancer (25–28). As an intravesically instilled agent, OGX427 monotherapy successfully reduced tumor volume, but there are no reports yet regarding intravesical combination treatment of ASO targeting Hsp27 and chemotherapeutic agents; more importantly, there are no previous studies comparing the efficacy of combination therapy of ASO therapeutics with chemotherapy versus chemotherapy alone when applied intravesically.

In the present study, we confirm the importance of Hsp27 as a molecular target to enhance chemosensitivity of bladder cancer and show effectiveness of combination treatment of ASO targeting Hsp27 and HTI-286 both *in vitro* and *in vivo*. These findings provide a novel strategy for intravesical treatment of patients with refractory nonmuscle-invasive bladder cancer.

Materials and Methods

Antibodies and Reagents

Antibodies were obtained as follows: anti-human HSP27 and anti-pp38 from StressGen; anti-pAkt, anti-p38, anti-Bax, and anti-human poly(ADP-ribose) polymerase from Cell Signaling Technology; anti-vinculin from Sigma; anti-Akt and anti–Bcl-2 from Santa Cruz Biotechnology; and anti–glyceraldehyde-3-phosphate dehydrogenase from Novus Biologicals. HTI-286 (*N*,β,β-trimethyl-L-phenylalanyl-*N*1-[(1*S*,2*E*)-3-carboxy-1-isopropylbut-2-enyl]-*N*1,3-dimethyl-L-valinamide, also known as SPA110 or taltobulin) was generously provided by Wyeth Research. HTI-286 powder was dissolved in DMSO to produce a stock solution of 10 mg/mL, which was then diluted in PBS or culture medium to obtain the desired concentrations before each experiment. Paclitaxel was purchased from Polymed Therapeutics, cisplatinum was from Sigma, and gemcitabine was kindly provided by the British Columbia Cancer Agency. OGX427, a second-generation ASO targeting Hsp27, was generously provided by OncoGeneX; the sequence of OGX427 corresponds to the translation initiation site of the human HSP27 gene (5-GGGACGCGGCGCTCGGTCAT-3). A scramble B (ScrB) control oligodeoxynucleotide was generously provided by ISIS Pharmaceuticals. LY294002 and SB203580 were obtained from Sigma-Aldrich.

Cell Culture

The human bladder cancer cell lines UMUC3 and T24 were purchased from the American Type Culture Collection. Cells were maintained in MEM or RPMI 1640 medium (Invitrogen) containing 10% fetal bovine serum and kept at 37°C in a humidified 5% CO_2 atmosphere, respectively. KK47 and 5637 cells were kindly provided by Dr. O. Ogawa (Kyoto University) and maintained in RPMI 1640 medium containing 10% fetal bovine serum. The KU7 cell line was kindly provided by Dr. M. Tachibana (Keio University). These cells were maintained in DMEM containing 5% fetal bovine serum and used for orthotopic model development. KU7 cells were infected with a lentivirus containing the firefly luciferase gene by Dr. Craig Logsdon (M. D. Anderson Cancer Center), and these subclones were named KU7-luc as described previously (7).

Lentiviral Infection of Hsp27 into T24 Cells

Human Hsp27cDNA was subcloned into the lentiviral vector pHR′-CMV-EGFP at the *Bam*HI and *Xho*I sites. Two vectors were created for study: pHR′-CMV-Hsp27 and pHR′-CMV (empty vector). Infectious lentivirus was generated by cotransfection of 1.5×10^6 293T cells with target plasmids with pCMVDR8.2 (carries the sequence necessary for viral assembly of lentivirus) and pMD.G that expresses the vesicular stomatitis virus envelope glycoprotein G pseudotype as described previously (21, 22). The 293T cells were transfected with Hsp27-expressing or empty lentiviral vector (10 μg of each) using the calcium phosphate precipitation method (Promega Profection Mammalian Transfection Systems). 293T cells were transfected for 12 to 15 h, after which fresh medium was added for 24 h. Following this, virus-containing media were collected and filtered through a 0.45 μm filter. T24 cells were plated in 10 cm plates, and competent retrovirus was added at a multiplicity of infection of 30 to 40. Cells were harvested after several passages, and whole-cell lysates were collected to ensure the expression of Hsp27 by Western blotting.

Cell Viability Assay

Cells were treated at 50% confluence with OGX427 or ScrB control at 50 nmol/L in serum-free Opti-MEM (Invitrogen) using Oligofectamine transfection reagent (Invitrogen). Four hours later, growth medium containing 15% or 30% fetal bovine serum was added, resulting in a final concentration of fetal bovine serum of 5% or 10%. Oligodeoxynucleotides were administered twice on 2 successive days, and cells were treated with indicated concentrations of each chemotherapeutic agent for 3 days. Cell viability was determined by 3-(4,5-dimethylthiazol-2-yl)-5-(3-carboxymethoxyphenyl)-2-(4-sulphophenyl)-2H-tetrazolium (MTS) assays. Briefly, MTS (Sigma-Aldrich) was combined with phenazine methosulfate in a ratio of 20:1. This mixture was added to the culture medium in a 1:5 ratio and incubated for 4 h at 37°C in a humidified 5% CO_2 atmosphere. Absorbance was read at 490 nm using a microplate reader (Becton Dickinson Labware).

RNA Isolation and Reverse Transcription-PCR

Total RNA was isolated from cultured bladder cancer cells using the Trizol method (Invitrogen). First-strand cDNA was synthesized from 2 μg total RNA using random primers according to the manufacturer's protocol (Invitrogen). Primer sequences used for MDR1 cDNA amplification were as follows: 5′-ATGTCCAACGTCCCCCACAAG-3′ (sense) and 5′-TGACGCGATGATGAGCACCTC-3′ (antisense), resulting in a 249-bp fragment. Primers for amplification of the housekeeping gene human β-actin were as follows: 5′-GGACCTGACTGACTACCTCATGAA-3′ (sense) and 5′-TGATCCACATCTGCTGGAAGGTGG-3′ (antisense), resulting in a 731-bp fragment. PCR regimen for MDR1 involved 5 min of initial denaturation at 95°C followed by 40 cycles at 94°C for 40 s, 54°C for 40 s, and 72°C for 1 min. PCR regimen for β-actin involved 5 min of initial denaturation at 94°C followed by 30 cycles at 94°C for 30 s, 62°C for 30 s, and 72°C for 1 min. PCR products were separated by electrophoresis on 2% agarose gels.

Western Blot Analysis

After drug treatments, cells were washed with PBS and lysed in an appropriate volume of ice-cold radioimmunoprecipitation assay buffer composed of 50 mmol/L Tris-HCl (pH 7.4), 150 mmol/L NaCl, 0.5% sodium deoxycholate, 1% NP-40, 0.1% SDS containing 1 mmol/L Na_3VO_4, 1 mmol/L NaF, 1 mmol/L phenylmethylsulfonyl fluoride, and protease inhibitor cocktail tablets (Complete; Roche Diagnostics). Cellular lysates were clarified by centrifugation at 13,000 × *g* for 20 min and protein concentrations of the lysates were determined by a BCA protein assay kit (Pierce). The lysates (10-30 μg) were boiled for 5 min in SDS sample buffer and separated by SDS-PAGE on a 10% to 15% Tris-HCl minigel and transferred onto a polyvinylidene difluoride membrane following standard methods. Membranes were probed with appropriate dilutions of primary antibodies followed by incubation with horseradish peroxidase–conjugated secondary antibodies. After extensive washing, proteins were visualized by a chemiluminescent detection system (GE Healthcare).

Cell Cycle Analysis

Flow cytometric analysis of propidium iodide–stained cells was done to determine their DNA profile for cell cycle analysis and to quantify apoptotic rates by detection of cells with sub-G_1 DNA content as reported previously (29). Briefly, after drug treatments, KU7 cells were trypsinized to produce a single-cell suspension and fixed with 70% ethanol. The next day, cells were washed with phosphate-citrate buffer to elute fragmented low-molecular-weight DNA and incubated with RNase A (0.5 mg/mL; Invitrogen) at 37°C for 30 min. Subsequently, cells were stained on ice with 1 mL of 50 μg/mL propidium iodide (Sigma-Aldrich), a fluorescent dye that intercalates double-stranded DNA. Relative DNA content was then analyzed on a dual-laser flow cytometer (Beckman Coulter Epics Elite; Beckman). Each assay was repeated thrice.

Tissue Microarray Immunohistochemistry

The BL803 tissue microarray was purchased from US Biomax. The BL803 tissue microarray contains 30 cases of transitional cell carcinoma, 5 each of tumor-adjacent tissue and normal tissue, duplicating cores per case. Each core measures 1.5 mm in diameter and cores are arrayed in rectangular fashion with a 10 × 8 layout. Each core from each cancer tissue represents one single specimen that was selected and pathologically confirmed. In addition to the BL803 tissue microarray, 11 cases BL801 tissue microarray (US Biomax), which contains 11 cases of normal bladder tissue was included, as was 5 clinical samples of carcinoma *in situ*. Therefore, in this study, we used 30 cases of transitional cell carcinoma with histologic grading and staging according to the WHO system (30) and 16 normal tissues to examine Hsp27 expression in bladder tissue. Immunohistochemical staining was conducted on a Ventana autostainer model Discover XT (Ventana Medical System) with an enzyme-labeled biotin streptavidin system and solvent-resistant DAB Map kit using a Hsp27 monoclonal antibody from Novacastra Labs. Tissue microarray slides were scanned on a BLISS System from Bacus Laboratories (Olympus). The staining intensity in each section was graded in a four-point visual scoring scheme (0-3 representing negative to high expression of Hsp27) with concern to the percentage of the area. All comparisons of staining intensity and percentages were made by a pathologist (L. Fazli) at ×20 magnification.

Orthotopic Murine Model of Bladder Cancer

The orthotopic mouse model used here was recently described by our group (7–11). Briefly, 8-week-old female Hsd: athymic nude-Foxn1nu mice (Harlan) were anesthetized with isoflurane. A superficial 6/0 polypropylene purse-string suture was placed around the urethral meatus before a lubricated 24-gauge Jelco angiocatheter (Medex Medical) was passed through the urethra into the bladder. After a single irrigation of the bladder with 100 μL PBS, 2 million KU7-luc cells were instilled as single-cell suspension in 50 μL, and the purse-string suture was tied down for a 2.5 h period, during which the mice were kept anesthetized. Five days after intravesical instillation of KU7-luc cells, orthotopic bladder tumor growth was confirmed via bioluminescence. Mice were then randomly divided into four groups. Treatment was done for 2 weeks as follows: (*a*) ScrB + DMSO (vehicle control), (*b*) ScrB + HTI-286, (*c*) OGX427 + DMSO, and (*d*) OGX427 + HTI-286. ScrB or OGX427 at 50 nmol/L was instilled three times per week, and DMSO or HTI-286 at 0.05 mg/mL in 50 μL was instilled biweekly. Both single-agent OGX427 and HTI-286 treatment was previously examined by our group in the same model, and the instilled doses and regimen of OGX427 and HTI-286 were decided according to those results (8, 9). To quantify *in vivo* tumor burden, animals were then imaged on days 5, 10, 15, 20, and 25 in an IVIS200 Imaging System (Caliper Life Sciences; see below). Necropsy was done after 25 days. The whole bladders were removed, fixed in 10% buffered formalin, and embedded in paraffin. At least one 5 μm section was obtained from each specimen and stained with H&E to assess morphology, and some were immunostained with Hsp27 using standard techniques described above. All slides were reviewed by a pathologist (L. Fazli) and were scanned on a BLISS workstation at magnification of ×5 to

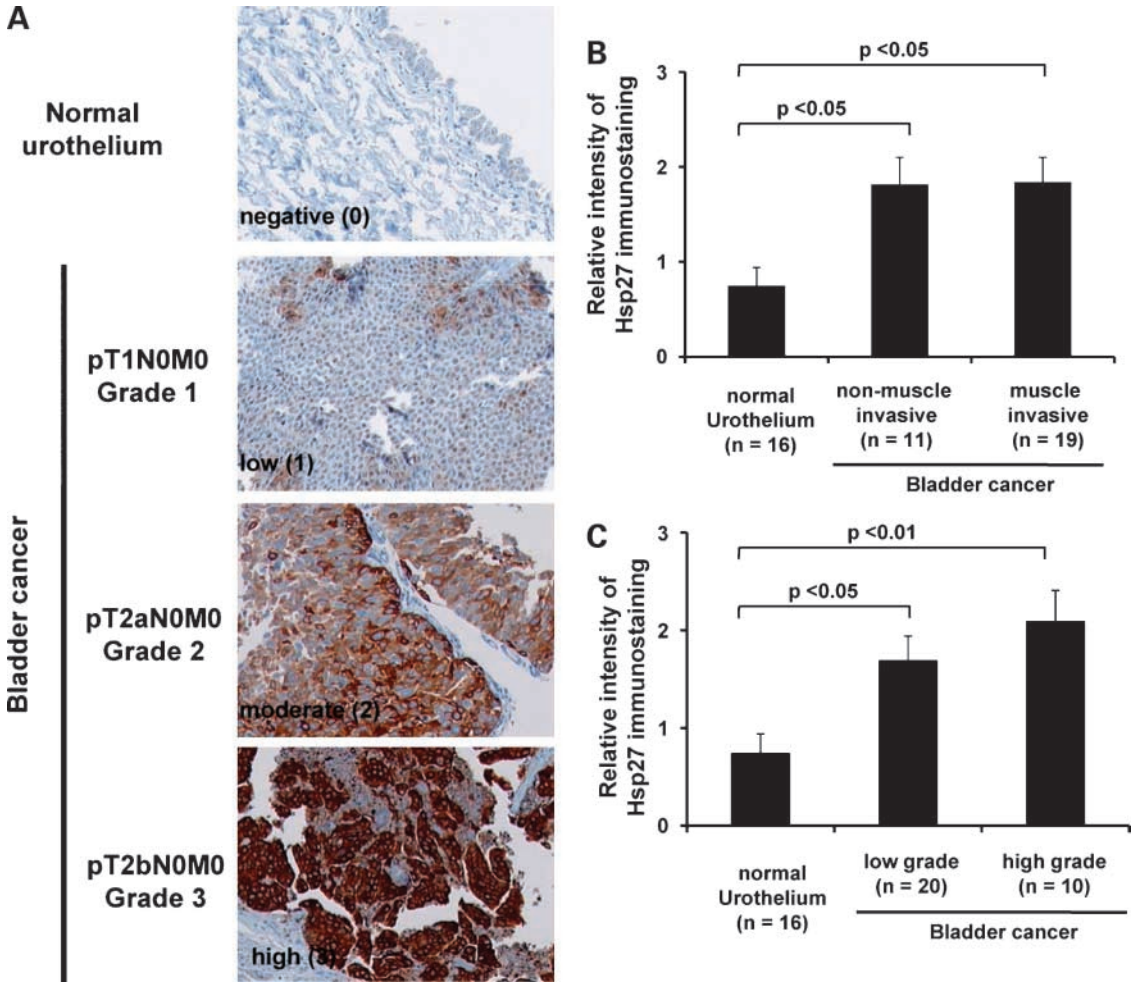

Figure 1. Hsp27 protein expression increases in bladder cancer tissue. **A,** immunohistochemical staining of Hsp27 in a human bladder cancer tissue microarray. Hsp27 levels were graded from 0 to +3 representing the range from no expression to high expression of Hsp27 by visual scoring. Four representative images show negative (0), low (1), moderate (2), and high (3) Hsp27 staining. **B,** immunostaining intensity of Hsp27 comparing normal bladder tissue (n = 5) and bladder cancer (n = 29). The grading score of Hsp27 expression from tissue microarray was calculated as mean ± SE and compared among normal bladder tissue and bladder cancer. **C,** immunostaining intensity of Hsp27 compared among normal bladder tissue, low-grade bladder cancer, and high-grade bladder cancer. The intensity was stratified into three groups consisting of negative, low to moderate, and high expression of Hsp27.

×20 (Bacus Laboratories). Animal procedures were done according to the guidelines of the Canadian Council on Animal Care.

Bioluminescence Imaging

Murine xenografts were imaged using an IVIS200 camera (Caliper Life Sciences). Briefly, mice were injected i.p. with 150 mg/kg D-luciferin (Caliper Life Sciences), anesthetized with isoflurane 5 min later, and imaged in the supine position exactly 11 and 15 min after injection. Then, the average of bioluminescence between 11 and 15 min was calculated. Data were acquired and analyzed using Living Image software version 3.0 (Caliper Life Sciences).

Statistical Analyses

All results are expressed as mean ± SE, calculated using Prism 4.03 (GraphPad Software). Data were analyzed by Kruskal-Wallis and Mann-Whitney U tests using InStat 3.06 (GraphPad). P values < 0.05 were considered statistically significant.

Results

Hsp27 is Highly Expressed in Human Bladder Cancer Specimen

As illustrated in Fig. 1, immunohistochemistry of human bladder cancer tissue microarrays revealed Hsp27 expression in 86.7% of tumors (26 of 30 tumors). Using a four-point scale, with 0 being no expression and 3 being high expression, there was no "high" expression of Hsp27 in normal urothelium compared with 36.7% of bladder tumors (11 tumors) expressing high levels of Hsp27, resulting in statistically significant difference of relative intensity of Hsp27 immunostaining (P = 0.0024). When Hsp27 expression was compared between non-muscle-invasive and

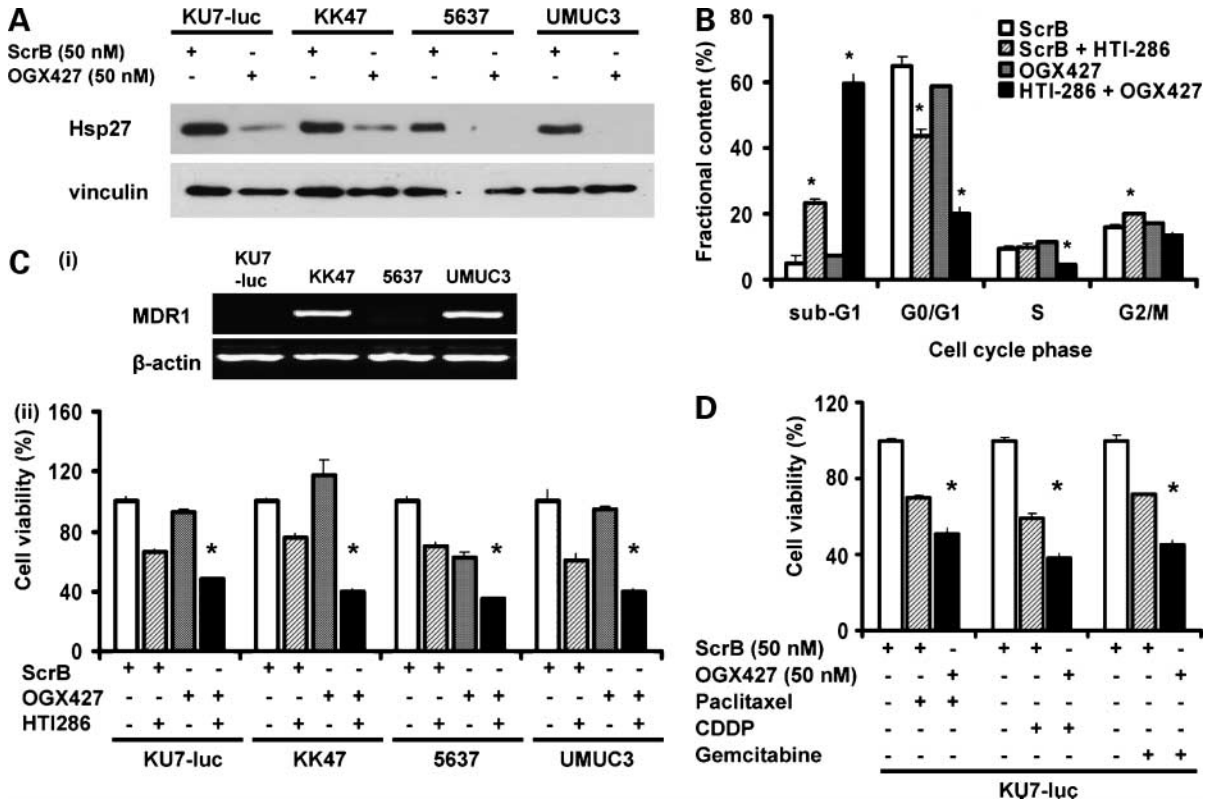

Figure 2. Suppression of Hsp27 protein enhances cytotoxicity in bladder cancer cells. **A,** sequence-specific suppression of Hsp27 protein levels by OGX427 in bladder cancer cells. Cells were treated with 50 nmol/L OGX427 or ScrB control oligodeoxynucleotide for 2 consecutive days; 72 h later, total protein was extracted and Hsp27 expression was analyzed by immunoblotting. **B,** flow cytometric analysis after treatment with OGX427and HTI-286. KU7-luc cells were treated with 50 nmol/L OGX427 or control oligodeoxynucleotide daily for 2 d. After 72 h of incubation with medium ± 0.6 nmol/L HTI-286, flow cytometry was used to quantify the percentage of cells in each cell cycle phase. *, $P < 0.05$. **C,** *i,* RT-PCR analysis showing MDR-1 expression in four different bladder cancer cell lines; *ii,* effects of OGX427 on HTI-286–induced cytotoxicity in bladder cancer cells. Cells were transfected with 50 nmol/L OGX427 or ScrB control oligodeoxynucleotide for 2 consecutive days and incubated with medium ± 0.5 nmol/L HTI-286 for 72 h. Cell viability was determined by MTS assays and is indicated by the ratio to cell viability when treated with drug vehicle only. *, $P < 0.05$. **D,** enhancement of various chemotherapeutic agents–induced cytotoxicity by OGX427 in KU7-luc cells. Cells were transfected with 50 nmol/L OGX427 or ScrB control oligodeoxynucleotide for 2 consecutive days and incubated with medium ± 20 nmol/L paclitaxel, 7.5 μmol/L cisplatinum (*CDDP*), or 10 nmol/L gemcitabine for 48 to 72 h. Cell viability was determined by MTS assays. *, $P < 0.05$.

muscle-invasive cancers, there was no difference in the mean intensity of Hsp27 immunostaining (1.8 ± 0.2959 versus 1.8 ± 0.2678), although both express significantly high Hsp27 compared with normal urothelium ($P < 0.05$; Fig. 1B). Furthermore, there was a clear tendency that Hsp27 expression was increased in high-grade bladder cancers (1.7 ± 0.2524 in low-grade bladder cancer and 2.1 ± 0.3145 in high-grade bladder cancer, respectively; Fig. 1C). These results show that, compared with normal bladder epithelium, Hsp27 is expressed at higher levels in bladder cancers, especially in high-grade bladder cancer independently of its muscle invasiveness.

Targeted Suppression of Hsp27 Enhances HTI-286–Induced Cytotoxicity in Bladder Cancer Cells

We then investigated the possibility of Hsp27 as a molecular target to enhance chemotherapy-induced cytotoxicity in bladder cancer cells. First, Western blot analysis was used to confirm knockdown of Hsp27 after OGX427 transfection in four different bladder cancer cell lines (Fig. 2A): treatment with 50 nmol/L OGX427 reduced Hsp27 expression levels in all four bladder cancer cell lines compared with ScrB control oligodeoxynucleotide. Next, to assess whether Hsp27 suppression alters chemosensitivity of bladder cancer cells to HTI-286, KU7-luc cells were treated with HTI-286 plus OGX427, and cell cycle distribution was examined by flow cytometric analysis. OGX427 monotherapy at 50 nmol/L did not induce apoptosis but greatly enhanced HTI-286–induced cytotoxicity and significantly increased the sub-G_1 population (Fig. 2B). The results of MTS assays also confirmed the effects of OGX427 to enhance HTI-286 cytotoxicity in four bladder cancer cell lines (Fig. 2C). Although two of four cell lines express MDR1, HTI-286 itself showed good cytotoxicity regardless of MDR1 expression, and the combination treatment with OGX427 further enhanced its chemotherapeutic efficacy. Furthermore, MTS assays showed that OGX427 enhanced the susceptibility not only to HTI-286 but also to other chemotherapeutic agents such as paclitaxel, cisplatinum, and gemcitabine in bladder cancer cells (Fig. 2D). These results indicate that suppression of Hsp27 chemosensitizes bladder cancer cells against several cytotoxic agents.

Suppression of Hsp27 Protein Inhibited Akt Phosphorylation and Induced Apoptosis Combined with HTI-286

Hsp27 has been reported to affect cisplatinum-induced cytotoxicity upstream of both ASK1/p38 apoptotic signaling and phosphatidylinositol 3-kinase/Akt survival signaling pathways (26). To investigate the molecular mechanisms underlying the effects of Hsp27 suppression enhancing HTI-286–induced cytotoxicity in KU7-luc bladder cancer cells, changes of those pathways were examined after HTI-286 and OGX427 treatment. Using Western blot analysis, OGX427 monotherapy did not remarkably change Akt or p38 phosphorylation, whereas combination treatment of OGX427 with HTI-286 suppressed Akt phosphorylation and induced p38 phosphorylation (Fig. 3A). Similarly, combination therapy suppressed Bcl-2 protein expression, whereas Bax protein levels did not change, leading to an increase of the Bax/Bcl-2 ratio. To examine the importance of p38 activation in this process, p38 activity was inhibited by SB203580, but this did not inhibit apoptosis when compared with treatments without the p38 inhibitor (Fig. 3B). Similarly, Akt inactivation was observed in KK47 cells treated with the combination of OGX427 and HTI-286 (Fig. 3C); furthermore, this was also observed when KU7-luc cells were treated by the combination of OGX427 and other chemotherapeutic agents (Fig. 3D).

Hsp27 Protects Bladder Cancer Cells from HTI-286–Induced Apoptosis by Enhancing HTI-286–Induced Akt Activation

To assess the protective effect of Hsp27 against drug-induced apoptosis, Hsp27-transfected T24 cells (T24 Hsp27) and empty vector-transfected T24 cells (T24 mock) were established (Fig. 4A), and their susceptibility to HTI-286 was compared. MTS assays show that T24 Hsp27 cells were more resistant to HTI-286 compared with T24 mock cells (Fig. 4A). At that time, Western blot analysis showed that Akt activation was more strongly induced by HTI-286 in T24 Hsp27 cells than in T24 mock cells, although there was no remarkable difference in the Akt phosphorylation level at the baseline (Fig. 4B). Similarly, poly(ADP-ribose) polymerase cleavage after HTI-286 treatment was reduced in T24 Hsp27 cells. Because the chemoresistance of T24 Hsp27 cells against HTI-286 decreased to a similar level as that of T24 mock cells after inhibition of Akt activity with LY294002,

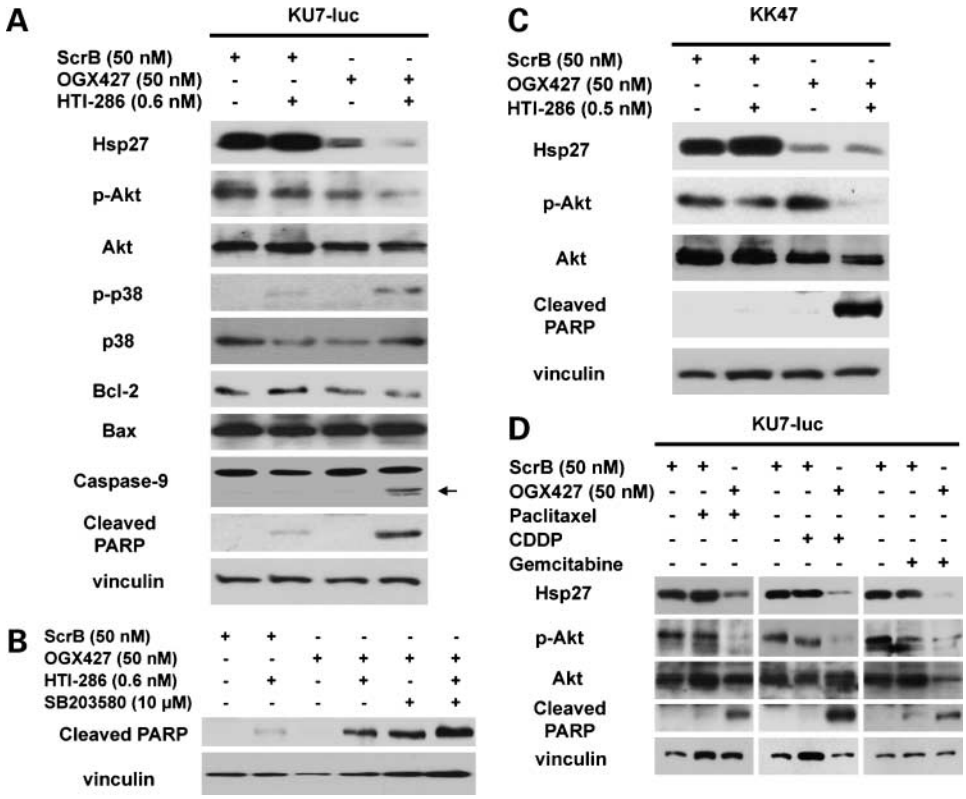

Figure 3. Suppression of Hsp27 combined with chemotherapeutic agents inactivated Akt signaling and promoted apoptosis. **A,** Western blot analysis showing the effects of combination treatment with OGX427 and HTI-286 in KU7-luc cells. Cells were treated as described in Fig. 2B and then subjected to Western blot analysis. *Black arrows,* cleaved forms of caspase-9 and poly(ADP-ribose) polymerase (*PARP*). **B,** effects of p38 inhibition on the susceptibility to HTI-286 and OGX427 of KU7-luc cells. Cells were transfected with 50 nmol/L OGX427 or ScrB control oligodeoxynucleotide for 2 consecutive days and incubated with medium ± 0.5 nmol/L HTI-286 and/or 10 μmol/L SB203580 for 72 h and then subjected to Western blot analysis. **C,** Western blot analysis showing the effects of combination treatment with OGX427 and HTI-286 in KK47 cells. Cells were treated as described in Fig. 2B and then subjected to Western blot analysis. **D,** Western blot analysis showing the effects of combination treatment with OGX427 and various chemotherapeutic agents in KU7-luc cells. Cells were treated as described in Fig. 2D and then subjected to Western blot analysis.

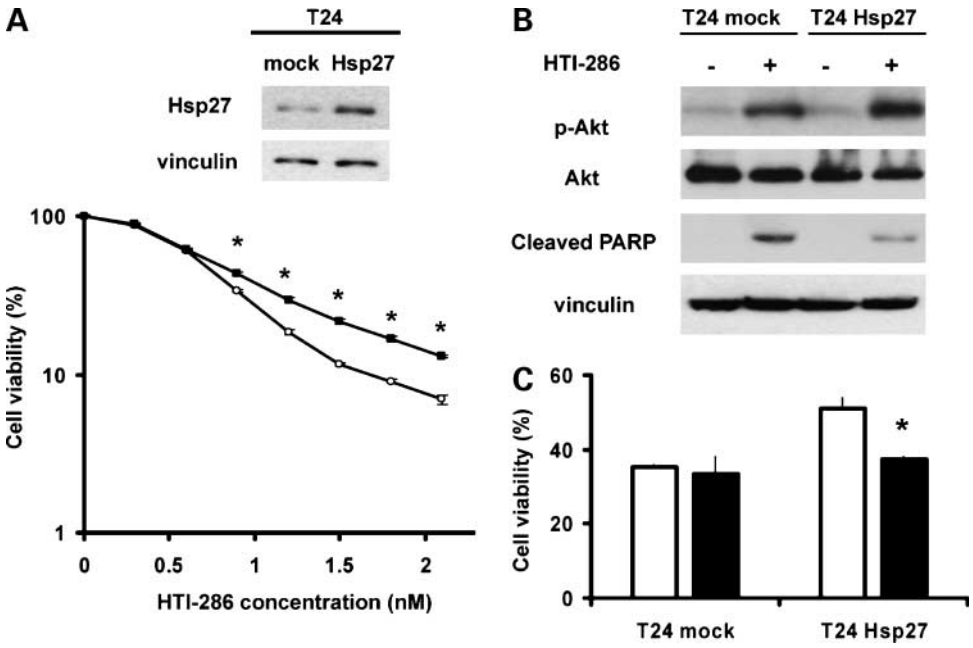

Figure 4. Overexpression of Hsp27 protein contributes to chemoresistance against HTI-286 in bladder cancer cells. **A,** *top,* expression level of Hsp27 in lysates harvested from T24 cells infected with empty lentiviral vector (mock) or Hsp27-expressing lentiviral vector (Hsp27). T24 cells were infected with lentivirus as described in Materials and Methods, and their cell lysates were subjected to Western blot analysis. *Bottom,* effect of overexpression of Hsp27 protein on the susceptibility to HTI-286 in T24 cells. The results of MTS assays of T24 mock (*open circles*) and T24 Hsp27 (*black squares*) treated with HTI-286 at the indicated concentrations for 72 h are shown as average ± SE from three independent experiments. Cell viability is indicated as the ratio to cell viability with no treatment. *, $P < 0.05$. **B,** induction of Akt activation and reduced poly(ADP-ribose) polymerase cleavage after HTI-286 treatment by Hsp27 overexpression. Cells were treated by 1.0 nmol/L HTI-286 or DMSO for 72 h and then lysed in radioimmunoprecipitation assay buffer and subjected to Western blot analysis. **C,** effects of Akt inactivation on the susceptibility to HTI-286 of T24 mock cells and T24 Hsp27 cells. Cells were treated by 1.0 nmol/L HTI-286 (*white column*) or HTI-286 + 20 μmol/L LY294002 (*black column*) for 72 h. Cell viability was determined by MTS assays and is indicated by the ratio to cell viability when treated with drug vehicle only. *, $P < 0.05$.

Akt activation was shown to be essential for the chemoresistance of T24 Hsp27 (Fig. 4C). Taken together, these results indicate that Hsp27 contributes to chemoresistance in bladder cancer cells via the Akt signaling pathway and modulation of Hsp27-Akt signaling may be the fundamental mechanism of OGX427 to enhance chemotherapeutic efficacy.

In vivo Hsp27 Knockdown by OGX427 Enhances the Sensitivity of Orthotopic Bladder Cancer to HTI-286

In vivo studies were done on 28 athymic nude mice to evaluate the efficacy of intravesical combination therapy. Regardless of the intravesical treatment given, neither significant changes in mice weight nor hematuria as a local adverse symptom were observed. Concerning antitumor efficacy, as early as on day 10, mice treated intravesically with ScrB + DMSO or with OGX427 + DMSO progressed significantly faster than mice treated by OGX427 + HTI-286 ($P = 0.0006$ and 0.0041, respectively; Fig. 5A and B). At the end of our study after 25 days, OGX427 and HTI-286 single-agent treatment only partially delayed tumor growth, whereas OGX427 + HTI-286 combination treatment significantly inhibited tumor growth compared with all other three treatment groups ($P = 0.0111$, 0.0379, and 0.0023 against ScrB + DMSO, ScrB + HTI-286 and OGX427 + DMSO, respectively). Western blot analysis and immunohistochemistry of mice bladders showed that intravesical treatment of OGX427 with DMSO or HTI-286 suppressed Hsp27 expression in superficial and deep layers of bladder tumors as described previously (ref. 9; Fig. 6A and B), although there was some heterogeneity in the extent of Hsp27 suppression among individual mice (data not shown). Furthermore, similar to our *in vitro* results, suppression of Akt phosphorylation was also observed in the combination treatment group (Fig. 6A and B).

Discussion

Intravesical BCG instillation is the most efficacious adjuvant regimen for non-muscle-invasive bladder cancer (6). However, BCG treatment frequently causes irritative voiding symptoms and, less frequently, systemic adverse events that may limit its use; in addition, BCG treatment is associated with a failure rate of 30% (4). Furthermore, conventional intravesical chemotherapy with cytotoxic agents such as mitomycin C or epirubicin lack evidence for long-term efficacy against high-risk bladder cancer. In this situation, antimicrotubule agents are expected to provide novel intravesical options and docetaxel exhibited promising efficacy in a phase I trial as a second-line intravesical agent for superficial bladder cancer refractory to standard therapy (31).

HTI-286, a fully synthetic analogue of the natural tripeptide hemiasterlin, interferes with spindle-microtubule dynamics leading to concentration-dependent apoptosis

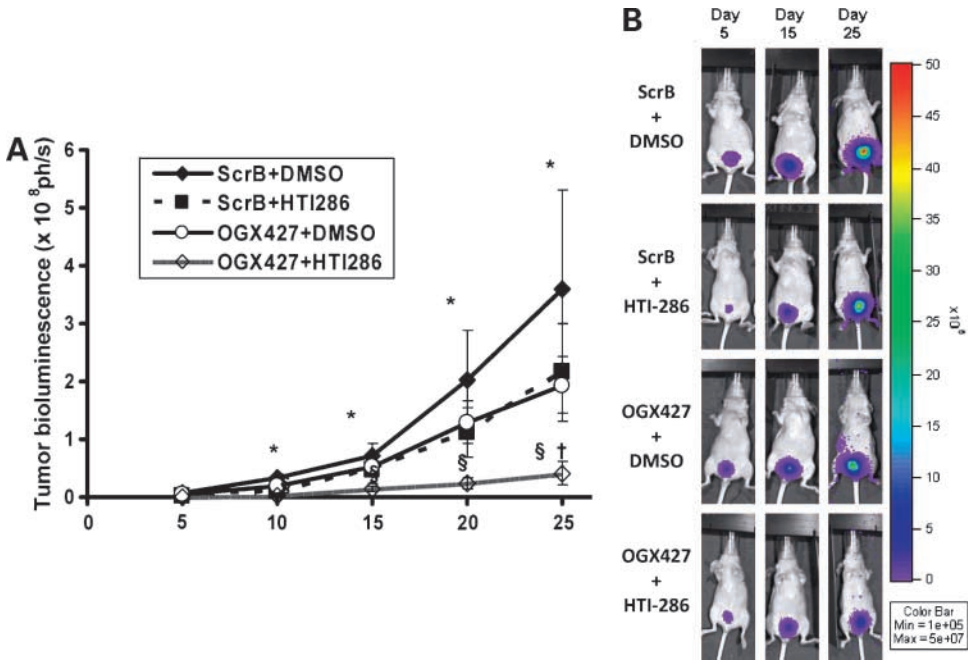

Figure 5. Intravesical instillation of HTI-286 and OGX427 suppresses the *in vivo* tumor growth on orthotopic bladder cancer xenografts. **A,** 28 female nude mice were inoculated with 2×10^6 KU7-luc tumor cells on day 0 and randomized on day 5 to receive either treatment with ScrB + DMSO, ScrB + HTI-286, OGX427 + DMSO, or OGX427 + HTI-286. ScrB or OGX427 was administered three times a week, and HTI-286 or DMSO was administered biweekly for 2 consecutive weeks. Tumor growth was determined on days 5, 10, 15, 20, and 25 in a Xenogen IVIS200 camera. *, $P < 0.05$, Kruskal Wallis test; †, $P < 0.05$, between ScrB + HTI-286 and OGX427 + HTI-286 groups; §, $P < 0.01$, between OGX427 + DMSO and OGX427 + HTI-286 groups, Mann-Whitney *U* tests. **B,** representative sequences of bioluminescence images of mice from each treatment group taken on the day of randomization (day 5) and at days 15 and 25.

(12–17). This chemotherapeutic has potent cytotoxic properties and may be useful in the setting of chemoresistance because it is a poor substrate for the efflux pump P-glycoprotein (18). Serretta et al. reported that P-glycoprotein was highly expressed among 50% of examined bladder cancer and its status was not modified by intravesical chemotherapy (32). The status of P-glycoprotein in bladder cancer correlates with chemoresistance when strongly expressed. Thus, HTI-286 may be used even in bladder cancers that express high levels of P-glycoprotein that are resistant to conventional chemotherapeutics, whether as primary or secondary therapy. Our previous data have shown that intravesical HTI-286 instillation therapy is efficacious against orthotopic bladder tumors, providing initial preclinical proof-of-principle for the use of HTI-286 against high-grade non-muscle-invasive bladder cancer (8). Issues that still require further evaluation include are pharmacokinetic properties of intravesically instilled HTI-286. Previous

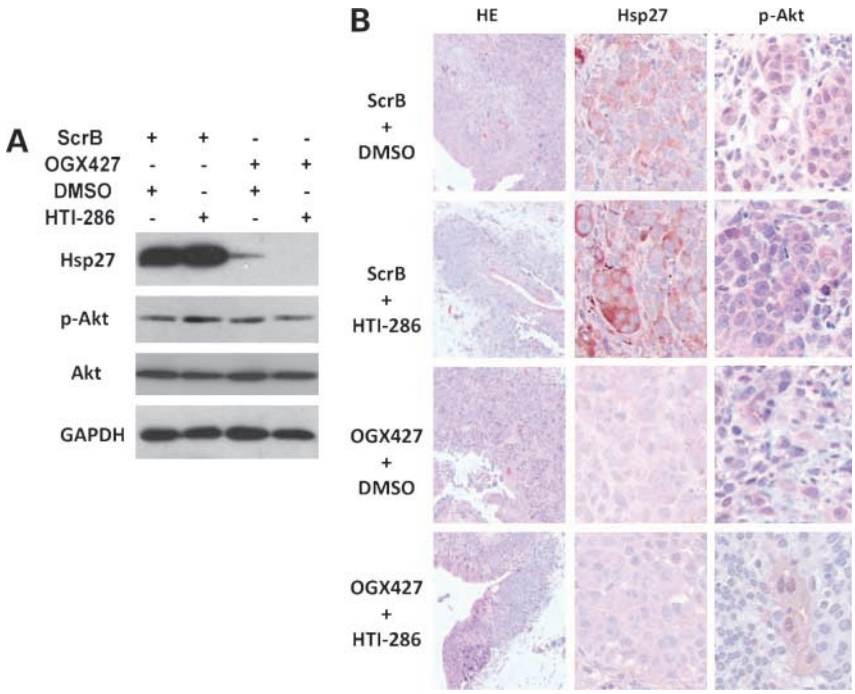

Figure 6. Intravesical instillation of HTI-286 and OGX427 suppresses the expression of Hsp27 and Akt activation on orthotopic bladder cancer xenografts. **A,** Western blot analysis showing representative Hsp27 or pAkt expression levels in mouse bladders. Protein was extracted from whole-bladder specimens of mice treated by indicated drugs and assessed by Western blot analysis. **B,** corresponding bladder immunohistochemistry of each treatment group. The bladders were removed on day 25, embedded in paraffin, and stained with H&E, Hsp27, and pAkt. Magnification, ×2.5 for H&E and ×10 for Hsp27 and pAkt on a BLISS workstation (Bacus Laboratories).

mouse pharmacokinetic studies showed low systemic uptake of HTI-286 with an estimated systemic bioavailability ~2% of the instilled dose, emphasizing the need to minimize the dose of intravesically instilled HTI-286 to as low as possible to minimize the amount of systemic absorption of the chemotherapeutic agent.

Hsp27 has been shown to be up-regulated in many malignancies, including prostate, liver, gastric, and breast cancers (21, 33–35). In bladder cancer, the prognostic significance of Hsp27 expression levels is still uncertain, but our results, which show that Hsp27 tended to be strongly expressed in bladder cancer tissue, support a previous study by Takashi et al. that reported that Hsp27 expression in bladder cancer is higher compared with normal tissue (23). From our results, Hsp27 seems to be highly expressed in high-grade bladder cancer independently of muscle invasiveness; therefore, our strategy targeting Hsp27 in combination treatment regimen appears to be reasonable as a molecular target therapy for high-grade non-muscle-invasive bladder cancer. Furthermore, ASO targeting antiapoptotic genes, such as Hsp27, clusterin, survivin, or Bcl-2, may be more effective in combination with antiproliferative drugs, because they suppress the cytoprotective response of cancer cells to increase the production of antiapoptotic proteins to overcome the apoptotic effects of chemotherapeutic agents. Following this rationale, although intravesical single-agent treatment with OGX427, a second-generation ASO targeting Hsp27, has shown some antitumor activity by itself (9), our most recent data clearly show that the combination treatment strategy of OGX427 with chemotherapeutic agents significantly suppressed bladder cancer growth both *in vitro* and *in vivo* greater than single-agent therapy regardless of the chemotherapy used (Fig. 2D).

Hsp27 protects cells from apoptosis via various mechanisms such as decreasing reactive oxygen species, restoring protein homeostasis, stabilizing the actin-cytoskeleton, delaying the release of cytochrome *c* from mitochondria and Bid intracellular redistribution, and inhibiting activation of caspase-3 (36–40). It has been reported that depression of drug-induced ASK1/p38 activation and enhancement of drug-induced Akt activation had a close relationship to Hsp27-induced chemoresistance against cisplatin (26). In our study, down-regulation of Hsp27 by OGX427 itself did not change p38 and Akt status, but, on the other hand, it induced both definitive p38 activation and Akt inactivation in combination with HTI-286 treatment. Because p38 inhibition by SB203580 did not suppress apoptosis evoked by combination treatment of OGX427 and HTI-286, we believe that p38 activation may not be a crucial mechanism to induce apoptosis after HTI-286 treatment. On the contrary, because chemoresistance against HTI-286 in T24 cells overexpressing Hsp27 was suppressed in the presence of the Akt inhibitor LY294002, interactions of Hsp27 and Akt signaling should be considered to be crucial for the enhancement of HTI-286–induced cytotoxicity by OGX427. This is consistent with results regarding Hsp27 and cisplatin reported by Zhang and Shen (26). These authors suggested that enhancement of Akt activation is associated with complex formation between Akt and Hsp27. Because there was no remarkable difference in the Akt phosphorylation level at the baseline between T24 mock and T24 Hsp27, we consider that Hsp27 may have a significant influence on Akt pathway especially when cancer cells are exposed to cellular stress. The mechanisms of Hsp27 to regulate Akt activity should be further elucidated in the future.

Although the mechanisms of Hsp27 to regulate Akt activity are still being evaluated, Akt has been reported to be upstream of various antiapoptotic or proapoptotic proteins. In our study, Bcl-2 down-regulation was observed when Akt was inactivated under combination therapy. Bcl-2 is tightly regulated by different mechanisms, including transcription, heterodimerization, and degradation, through the ubiquitin-proteasome pathway and Akt has a close relationship to regulate Bcl-2 function through those steps. One of the interacting mechanisms is the inactivation of Bad by Akt, which disrupts Bad-Bcl-2 complexes and then makes Bcl-2 free to act as an antiapoptotic effector (41). Furthermore, Akt is also involved in transcriptional regulation of Bcl-2, and inhibition of Akt activity has been reported to significantly decrease Bcl-2 promoter activity (42). Although Havasi et al. suggested the possibility that Hsp27-mediated changes of Akt regulate Bax activity through GSK3β (43), changes in Bcl-2 expression might also contribute to the control of Bax activity by Akt.

Despite our analyzing the molecular mechanisms by which our combination therapy induced apoptosis in cancer cells *in vitro*, there are some limitations to our *in vivo* study. Our pharmacokinetic analysis of oligodeoxynucleotide uptake was limited, and we did not include pharmacokinetic analyses of HTI-286 uptake using high-performance liquid chromatography-mass spectrometry. However, previous pharmacokinetic analyses of intravesical OGX427 and HTI-286 when given independently resulted in minimal systemic absorption (8, 9). Furthermore, we think that it may be difficult to compare the effect of this combination treatment with conventional BCG treatment in the preclinical model, because an immunocompetent model to examine the effect of BCG treatment is required. A phase I clinical trial to compare the effect of combination of these treatments to assess adverse effects as well as pharmacokinetic and pharmacodynamic profiles is required.

In conclusion, our studies suggest that interaction of Hsp27 with the Akt pathway may be an important molecular target to enhance chemotherapeutic efficacy of HTI-286. Our *in vitro* and *in vivo* data provide strong preclinical proof-of-principle for the use of a novel intravesical combination treatment consisting of OGX427 and HTI-286 for high-grade bladder cancer with Hsp27 overexpression. Although OGX427 is already in phase I clinical trials both as an intravenous single-agent and in combination with docetaxel in patients with advanced prostate, ovarian, lung, breast, or bladder cancers, further research is warranted to evaluate the efficacy and safety of intravesical combination treatment of OGX427 with other chemotherapeutic agents such as HTI-286.

Disclosure of Potential Conflicts of Interest

R.J. Andersen: inventor on patent for HTI-286, which has been licensed from the University of British Columbia to Wyeth Pharmaceuticals. M.E. Gleave: cofounder and CSO, OncoGeneX. No other potential conflicts of interest were disclosed.

Acknowledgments

We thank Estelle Li, Lydia Liao, and Ada Leung for the excellent technical assistance.

References

1. Jemal A, Siegel R, Ward E, et al. Cancer statistics, 2008. CA Cancer J Clin 2008;58:71–96.

2. Clark PE. Bladder cancer. Curr Opin Oncol 2007;19:241–7.

3. Dalbagni G. The management of superficial bladder cancer. Nat Clin Pract Urol 2007;4:254–60.

4. Cookson MS, Herr HW, Zhang ZF, Soloway S, Sogani PC, Fair WR. The treated natural history of high risk superficial bladder cancer: 15-year outcome. J Urol 1997;158:62–7.

5. Shahin O, Thalmann GN, Rentsch C, Mazzucchelli L, Studer UE. A retrospective analysis of 153 patients treated with or without intravesical bacillus Calmette-Guerin for primary stage T_1 grade 3 bladder cancer: recurrence, progression and survival. J Urol 2003;169:96–100; discussion.

6. Sylvester RJ, van der MA, Lamm DL. Intravesical bacillus Calmette-Guerin reduces the risk of progression in patients with superficial bladder cancer: a meta-analysis of the published results of randomized clinical trials. J Urol 2002;168:1964–70.

7. Hadaschik BA, Black PC, Sea JC, et al. A validated mouse model for orthotopic bladder cancer using transurethral tumour inoculation and bioluminescence imaging. BJU Int 2007;100:1377–84.

8. Hadaschik BA, Adomat H, Fazli L, et al. Intravesical chemotherapy of high-grade bladder cancer with HTI-286, a synthetic analogue of the marine sponge product hemiasterlin. Clin Cancer Res 2008;14:1510–8.

9. Hadaschik BA, Jackson J, Fazli L, et al. Intravesically administered antisense oligonucleotides targeting heat-shock protein-27 inhibit the growth of non-muscle-invasive bladder cancer. BJU Int 2008;102:610–6.

10. Hadaschik BA, ter Borg MG, Jackson J, et al. Paclitaxel and cisplatin as intravesical agents against non-muscle-invasive bladder cancer. BJU Int 2008;101:1347–55.

11. Hadaschik BA, Zhang K, So AI, et al. Oncolytic vesicular stomatitis viruses are potent agents for intravesical treatment of high-risk bladder cancer. Cancer Res 2008;68:4506–10.

12. Nieman JA, Coleman JE, Wallace DJ, et al. Synthesis and antimitotic/cytotoxic activity of hemiasterlin analogues. J Nat Prod 2003;66:183–99.

13. Zask A, Birnberg G, Cheung K, et al. Synthesis and biological activity of analogues of the antimicrotubule agent *N*,β,β-trimethyl-L-phenylalanyl-*N*(1)-[(1*S*,2*E*)-3-carboxy-1-isopropylbut-2-enyl]-*N*(1),3-dimethyl-L-valinamide (HTI-286). J Med Chem 2004;47:4774–86.

14. Nunes M, Kaplan J, Wooters J, et al. Two photoaffinity analogues of the tripeptide, hemiasterlin, exclusively label α-tubulin. Biochemistry 2005;44:6844–57.

15. Ravi M, Zask A, Rush TS, III. Structure-based identification of the binding site for the hemiasterlin analogue HTI-286 on tubulin. Biochemistry 2005;44:15871–9.

16. Jordan MA, Wilson L. Microtubules as a target for anticancer drugs. Nat Rev Cancer 2004;4:253–65.

17. Anderson HJ, Coleman JE, Andersen RJ, Roberge M. Cytotoxic peptides hemiasterlin, hemiasterlin A and hemiasterlin B induce mitotic arrest and abnormal spindle formation. Cancer Chemother Pharmacol 1997;39:223–6.

18. Loganzo F, Discafani CM, Annable T, et al. HTI-286, a synthetic analogue of the tripeptide hemiasterlin, is a potent antimicrotubule agent that circumvents P-glycoprotein-mediated resistance *in vitro* and *in vivo*. Cancer Res 2003;63:1838–45.

19. Dang LH, Bettegowda C, Agrawal N, et al. Targeting vascular and avascular compartments of tumors with *C. novyi*-NT and anti-microtubule agents. Cancer Biol Ther 2004;3:326–37.

20. Venook AP, Enders Klein C, Fleming G, et al. A phase I and pharmacokinetic study of irinotecan in patients with hepatic or renal dysfunction or with prior pelvic radiation: CALGB 9863. Ann Oncol 2003;14:1783–90.

21. Ciocca DR, Calderwood SK. Heat shock proteins in cancer: diagnostic, prognostic, predictive, and treatment implications. Cell Stress Chaperones 2005;10:86–103.

22. Concannon CG, Gorman AM, Samali A. On the role of Hsp27 in regulating apoptosis. Apoptosis 2003;8:61–70.

23. Takashi M, Katsuno S, Sakata T, Ohshima S, Kato K. Different concentrations of two small stress proteins, αB crystallin and HSP27 in human urological tumor tissues. Urol Res 1998;26:395–9.

24. Lebret T, Watson RW, Molinie V, et al. Heat shock proteins HSP27, HSP60, HSP70, and HSP90: expression in bladder carcinoma. Cancer 2003;98:970–7.

25. McCollum AK, Teneyck CJ, Sauer BM, Toft DO, Erlichman C. Up-regulation of heat shock protein 27 induces resistance to 17-allylamino-demethoxygeldanamycin through a glutathione-mediated mechanism. Cancer Res 2006;66:10967–75.

26. Zhang Y, Shen X. Heat shock protein 27 protects L929 cells from cisplatin-induced apoptosis by enhancing Akt activation and abating suppression of thioredoxin reductase activity. Clin Cancer Res 2007;13:2855–64.

27. Kamada M, So A, Muramaki M, Rocchi P, Beraldi E, Gleave M. Hsp27 knockdown using nucleotide-based therapies inhibit tumor growth and enhance chemotherapy in human bladder cancer cells. Mol Cancer Ther 2007;6:299–308.

28. Rocchi P, So A, Kojima S, et al. Heat shock protein 27 increases after androgen ablation and plays a cytoprotective role in hormone-refractory prostate cancer. Cancer Res 2004;64:6595–602.

29. Zellweger T, Chi K, Miyake H, et al. Enhanced radiation sensitivity in prostate cancer by inhibition of the cell survival protein clusterin. Clin Cancer Res 2002;8:3276–84.

30. Sobin LH, Fleming ID. TNM classification of malignant tumors, fifth edition (1997). Union Internationale Contre le Cancer and the American Joint Committee on Cancer. Cancer 1997;80:1803–4.

31. McKiernan JM, Masson P, Murphy AM, et al. Phase I trial of intravesical docetaxel in the management of superficial bladder cancer refractory to standard intravesical therapy. J Clin Oncol 2006;24:3075–80.

32. Serretta V, Pavone C, Allegro R, et al. Correlation between GP-170 expression, prognosis, and chemoresistance of superficial bladder carcinoma. J Cancer Res Clin Oncol 2003;129:472–6.

33. Kapranos N, Kominea A, Konstantinopoulos PA, et al. Expression of the 27-kDa heat shock protein (HSP27) in gastric carcinomas and adjacent normal, metaplastic, and dysplastic gastric mucosa, and its prognostic significance. J Cancer Res Clin Oncol 2002;128:426–32.

34. Arts HJ, Hollema H, Lemstra W, et al. Heat-shock-protein-27 (Hsp27) expression in ovarian carcinoma: relation in response to chemotherapy and prognosis. Int J Cancer 1999;84:234–8.

35. van de Vijver MJ, He YD, van't Veer LJ, et al. A gene-expression signature as a predictor of survival in breast cancer. N Engl J Med 2002;347:1999–2009.

36. Garrido C, Ottavi P, Fromentin A, et al. HSP27 as a mediator of confluence-dependent resistance to cell death induced by anticancer drugs. Cancer Res 1997;57:2661–7.

37. Jolly C, Morimoto RI. Role of the heat shock response and molecular chaperones in oncogenesis and cell death. J Natl Cancer Inst 2000;92:1564–72.

38. Richards EH, Hickey E, Weber L, Master JR. Effect of overexpression of the small heat shock protein HSP27 on the heat and drug sensitivities of human testis tumor cells. Cancer Res 1996;56:2446–51.

39. Paul C, Manero F, Gonin S, Kretz-Remy C, Virot S, Arrigo AP. Hsp27 as a negative regulator of cytochrome *c* release. Mol Cell Biol 2002;22:816–34.

40. Xanthoudakis S, Nicholson DW. Heat-shock proteins as death determinants. Nat Cell Biol 2000;2:E163–5.

41. Blume-Jensen P, Janknecht R, Hunter T. The kit receptor promotes cell survival via activation of PI 3-kinase and subsequent Akt-mediated phosphorylation of Bad on Ser^{136}. Curr Biol 1998;8:779–82.

42. Pugazhenthi S, Nesterova A, Sable C, et al. Akt/protein kinase B up-regulates Bcl-2 expression through cAMP-response element-binding protein. J Biol Chem 2000;275:10761–6.

43. Havasi A, Li Z, Wang Z, et al. Hsp27 inhibits Bax activation and apoptosis via a phosphatidylinositol 3-kinase-dependent mechanism. J Biol Chem 2008;283:12305–13.